Asymmetric OFDM Systems Based on Layered FFT Structure

Jian (Andrew) Zhang, *Member, IEEE*, A. D. S. Jayalath, *Member, IEEE*, and Ying Chen, *Student Member, IEEE*

***Abstract*—In this letter, we first extend the convolution theory of discrete Fourier transform (DFT) and introduce a structure of layered fast Fourier transform (FFT). Based on this framework, we propose novel asymmetric orthogonal frequency-division multiplexing (OFDM) systems that bridge general OFDM and single carrier systems. Adaptive to the capability of the transceiver, asymmetric OFDM systems provide significant flexibility in system design and operation. We show how effects of noise enhancement and frequency diversity counteract each other in asymmetric OFDM systems. Performance comparison with general OFDM and single carrier systems is also given.**

***Index Terms*—Fast Fourier transform (FFT), frequency diversity, orthogonal frequency-division multiplexing (OFDM), peak-to-average power ratio (PAPR).**

I. Introduction

ORTHOGONAL frequency-division multiplexing (OFDM) is a spectrum-efficient signalling scheme to combat dense multipath channels for broadband wireless communications. However, OFDM systems also suffer from well-known problems including large peak-to-average power ratio (PAPR) [1] and sensitivity to carrier frequency offset (CFO) [2]. As an alternative solution, frequency-domain equalized single carrier system (SC-FDE) [3] retains OFDM's capability of combating multipath while mitigating the PAPR and frequency offset sensitivity problems. However, one problem with SC-FDE systems is that the complexity in the transmitter and receiver is very unbalanced. In this letter, we present asymmetric OFDM systems that bridge the gap between general OFDM and SC-FDE systems. The systems are developed based on a novel "*layered*" fast Fourier transform (FFT) structure that is an extension of the convolution property of the discrete Fourier transform (DFT) [4]. The proposed asymmetric OFDM systems provide flexibility in system design and operation by adapting to the capability of the transceiver, such as the dynamic range of power amplifier and battery status, and duplex requirements.

Notations: In this letter, symbols belonging to different layers are represented with different accents: $\tilde{x}$ for a frequency-domain symbol x, $\breve{x}$ for an intermediate layer symbol x, and time-domain symbols have no accent.

Manuscript received April 11, 2007; revised May 22, 2007. National ICT Australia is funded by the Australian Government's Backing Australia's Ability initiative, in part through the Australian Research Council. The associate editor coordinating the review of this manuscript and approving it for publication was Dr. Stefano Galli.

The authors are with the Wireless Signal Processing Program, National ICT Australia (NICTA), Canberra 2612, Australia, and also with the Australian National University (e-mail: Andrew.Zhang@nicta.com.au; Dhammika.Jayalath@nicta.com.au; Ying.Chen@nicta.com.au).

Color versions of one or more of the figures in this paper are available online at http://ieeexplore.ieee.org.

Digital Object Identifier 10.1109/LSP.2007.903230

II. Layered FFT Structure

It is well known that the divide-and-conquer (D&C) algorithm is the basis of FFT algorithms to compute the DFT. Below, we recall the process of the D&C algorithm to calculate an N-point DFT of the signal $\mathbf{x} = \{x_i\}$, $i = 0, 1, \ldots, N-1$.

S1) Stack the input signal $\mathbf{x} = \{x_i\}$, $i = 0, 1, \ldots, N-1$ column-wise into a $P \times Q$ matrix $\mathbf{X} = \{x_{p,q}\}$, $p \in [0, P-1]$, $q \in [0, Q-1]$ with $x_{p,q} = x_{qP+p}$ and $N = PQ$.

S2) Compute the Q-point DFTs for each row of $\mathbf{X}$, and yield a new matrix $\breve{\mathbf{X}} = \{\breve{x}_{l,q}\}$, $l = 0, 1, \ldots, P-1$, $q = 0, 1, \ldots, Q-1$ with $\breve{x}_{l,q} = \sum_{m=0}^{Q-1} x_{l,m} W_Q^{mq}$, $q \in [0, Q-1]$, where $W_Q = \exp(-j2\pi/Q)$.

S3) Multiply $\breve{\mathbf{X}}$ by the phase factors W_N^{lq}, where $W_N = \exp(-j2\pi/N)$, and generate a new matrix $\tilde{\mathbf{V}} = \{\tilde{v}_{l,q}\}$ with $\tilde{v}_{l,q} = W_N^{lq} \breve{x}_{l,q}$.

S4) Compute the P-point DFTs for each column of $\tilde{\mathbf{V}}$, and we get $\tilde{\mathbf{x}}_q = (\tilde{x}_{0,q}, \tilde{x}_{1,q}, \ldots, \tilde{x}_{P-1,q})^T$ with

$$\tilde{x}_{p,q} = \sum_{l=0}^{P-1} \tilde{v}_{l,q} W_P^{lp} = \sum_{l=0}^{P-1} \left(\breve{x}_{l,q} W_N^{lq} \right) W_P^{lp}. \tag{1}$$

S5) Read the resulting $P \times Q$ matrix $\tilde{\mathbf{X}} = \{\tilde{x}_{p,q}\}$ row-wise, and the resulting output is the DFT of $\mathbf{x}$, $\tilde{\mathbf{x}} = \{\tilde{x}_i\}$, $i = 0, 1, \ldots, N-1$, with $\tilde{x}_{pQ+q} = \tilde{x}_{p,q}$.

Given two N-point signals $\mathbf{x}$, $\mathbf{h}$, and their circular convolution output $\mathbf{y} = \mathbf{x} \circledast \mathbf{h}$, we know that their DFTs have the relationship $\tilde{\mathbf{y}} = \tilde{\mathbf{x}} \odot \tilde{\mathbf{h}}$, where $\circledast$ and $\odot$ denote the circular convolution and element-wise product of two vectors, respectively. Now let us consider the relationship between the intermediate outputs, that is, the per-row DFT outputs in Step S2, in the D&C approach for $\mathbf{x}$, $\mathbf{h}$, and $\mathbf{y}$.

If we rearrange the frequency domain samples $\tilde{\mathbf{x}}$, $\tilde{\mathbf{h}}$, and $\tilde{\mathbf{y}}$ into $P \times Q$ matrices row-wise according to the reverse process of S5 in the D&C approach, we get matrices $\tilde{\mathbf{X}} = \{\tilde{\mathbf{x}}_q\}$, $\tilde{\mathbf{H}} = \{\tilde{\mathbf{h}}_q\}$, $\tilde{\mathbf{Y}} = \{\tilde{\mathbf{y}}_q\}$, $q = 0, 1, \ldots, Q-1$, with respective qth column vector

$$\tilde{\mathbf{x}}_q = (\tilde{x}_{0,q}, \ldots, \tilde{x}_{p,q}, \ldots, \tilde{x}_{P-1,q})^T, \quad \tilde{x}_{p,q} = \tilde{x}_{pQ+q} \tag{2}$$

$$\tilde{\mathbf{h}}_q = (\tilde{h}_{0,q}, \ldots, \tilde{h}_{p,q}, \ldots, \tilde{h}_{P-1,q})^T, \quad \tilde{h}_{p,q} = \tilde{h}_{pQ+q} \tag{3}$$

$$\tilde{\mathbf{y}}_q = (\tilde{y}_{0,q}, \ldots, \tilde{y}_{p,q}, \ldots, \tilde{y}_{P-1,q})^T, \quad \tilde{y}_{p,q} = \tilde{y}_{pQ+q} \tag{4}$$

$p = 0, 1, \ldots, P-1$.

The reformatted frequency domain vectors retain the multiplication relationship $\tilde{\mathbf{y}}_q = \tilde{\mathbf{x}}_q \odot \tilde{\mathbf{h}}_q$. From (1), according to the convolution property of DFT, it is straightforward to see that for any $q \in [0, Q-1]$, the vector $\left\{ \breve{y}_{l,q} W_N^{lq} \right\}$ equals to the length-P circular convolution of the two vectors $\left\{ \breve{x}_{l,q} W_N^{lq} \right\}$

and $\left\{\breve{h}_{l,q}W_N^{lq}\right\}$, $l=0,1,\ldots,P-1$. Thus, the lth element in $\left\{\breve{y}_{l,q}W_N^{lq}\right\}$ can be represented as

$$\breve{y}_{l,q}W_N^{lq}=\sum_{m=0}^{P-1}\breve{x}_{m,q}W_N^{mq}\breve{h}_{((l-m))_P,q}W_N^{q((l-m))_P} \quad (5)$$

where $((l-m))_P$ denotes $(l-m)$ modulo P. Thus, for any $q\in[0,Q-1]$, we have

$$\breve{y}_{l,q}=\sum_{m=0}^{l}\breve{x}_{m,q}\breve{h}_{(l-m),q}+\sum_{m=l+1}^{P-1}\breve{x}_{m,q}\breve{h}_{(P+l-m),q}W_Q^q \quad (6)$$

where $l=0,1,\ldots,P-1$. Equation (6) establishes the relationship of the intermediate outputs in the D&C approach. The equation can also be expressed in matrix form. To summarize, we have the following theorem.

Theorem 1: For two N-point discrete signals $\mathbf{x}$ and $\mathbf{h}$ and their circular convolution $\mathbf{y}$, their intermediate outputs, per-row DFT outputs in the columnwise divide-and-conquer algorithm, are connected by

$$\breve{\mathbf{y}}_q=\breve{\mathbf{H}}_q\breve{\mathbf{x}}_q \quad (7)$$

where $\breve{\mathbf{y}}_q$, $\breve{\mathbf{x}}_q$, and $\breve{\mathbf{H}}_q$ are defined as

$$\breve{\mathbf{y}}_q=(\breve{y}_{0,q},\breve{y}_{1,q},\breve{y}_{2,q},\ldots,\breve{y}_{P-1,q})^T \quad (8)$$

$$\breve{\mathbf{x}}_q=(\breve{x}_{0,q},\breve{x}_{1,q},\breve{x}_{2,q},\ldots,\breve{x}_{P-1,q})^T \quad (9)$$

$$\breve{\mathbf{H}}_q=\begin{pmatrix}\breve{h}_{0,q} & W_Q^q\breve{h}_{P-1,q} & \cdots & W_Q^q\breve{h}_{1,q}\\ \breve{h}_{1,q} & \breve{h}_{0,q} & \cdots & W_Q^q\breve{h}_{2,q}\\ \vdots & \vdots & \ddots & \vdots\\ \breve{h}_{P-1,q} & \breve{h}_{P-2,q} & \cdots & \breve{h}_{0,q}\end{pmatrix} \quad (10)$$

respectively.

Together with the circular convolution property of DFT, we see a three-layer FFT structure: the input layer (time-domain signals), the intermediate layer (per-row DFT outputs), and the output layer (final frequency-domain signals). As an extension to the general two-layer FFT structure (time domain and frequency domain), this three-layer FFT structure provides more flexibility in system design. By letting the inputs be in the intermediate layer instead of the frequency-domain or time-domain layers, we can develop, for example, the following asymmetric OFDM system that bridges general OFDM and SC-FDE systems.

III. Asymmetric OFDM Systems

According to Theorem 1, we can see that OFDM and SC-FDE systems correspond to $P=1$ and $P=N$, respectively. We can design asymmetric OFDM systems by choosing any factor P of N, preferably a power of 2 for implementation convenience, and letting $\breve{\mathbf{x}}_q$, $q=0,1,\ldots,N/P-1$ be the inputs. The value of P can be negotiated between the transmitter and receiver according to their power supply, hardware capability (linearity of power amplifier, capability of FFT module, etc.), and duplex requirement. The baseband structure of the proposed asymmetric OFDM system is shown in Fig. 1.

At the transmitter, input data are first coded, interleaved, and modulated and then arranged into an $P\times Q$ array. The data in the qth column of the array are denoted as vector $\breve{\mathbf{x}}_q$. A Q-point IFFT is then applied to each row. Under the assumption that the IFFT outputs are stored in the same array, then the outputs are read out column-wise. In practical systems, this can be realized by a $P\times Q$ rectangular interleaver. The output of the interleaver is appended with a cyclic prefix (or zero padding). The signal is transmitted over a channel with a digital tap-delayed line (TDL) model $\mathbf{h}=(h_0,h_1,\ldots,h_{L-1})$. The channel is assumed to be quasi-static, being constant over at least one OFDM symbol period.

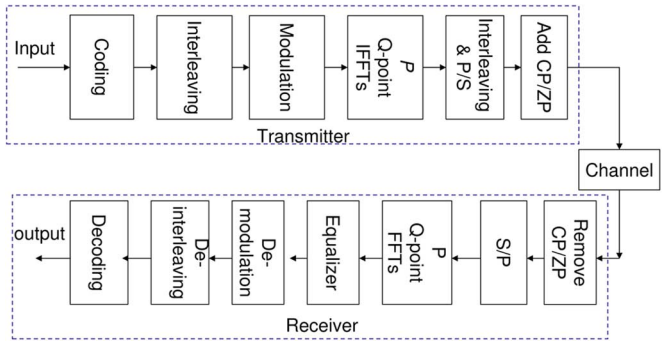

Fig. 1. Block diagram of the proposed asymmetric OFDM systems.

At the receiver, after removing the cyclic prefix, the samples are input column-wise to a $P\times Q$ array. A Q-point FFT is applied to each row. Assume the FFT outputs are stored in the same array, and denote the FFT outputs in the qth column as $\breve{\mathbf{y}}_q$. Now $\breve{\mathbf{y}}_q$ and $\breve{\mathbf{x}}_q$ have the relationship of

$$\breve{\mathbf{y}}_q=\breve{\mathbf{H}}_q\breve{\mathbf{x}}_q+\breve{\mathbf{n}}_q \quad (11)$$

where $\breve{\mathbf{H}}_q$ is the channel matrix defined in (10), $\breve{\mathbf{n}}_q$ contain AWGN samples, each having zero mean and variance σ_n^2. Note that the samples in $\breve{\mathbf{n}}_q$ have the same mean and variance as the noise samples introduced in the received time-domain signals, because the FFT does not change the statistical property of the AWGN.

Instead of directly computing the inverse of $\breve{\mathbf{H}}_q$, we derive the following efficient algorithm that enables simple one-tap equalization as used in OFDM systems. Observe that $\breve{\mathbf{H}}_q$ is a factor-circulant matrix [5], which can be diagonalized as

$$\mathbf{D}_q=\mathbf{F}_P\Phi_q^{-1}\breve{\mathbf{H}}_q\Phi_q\mathbf{F}_P^H \quad (12)$$

where Φ_q is a diagonal matrix

$$\Phi_q=\operatorname{diag}\left(1,W_N^{-q},W_N^{-2q},\ldots,W_N^{-(P-1)q}\right) \quad (13)$$

$\mathbf{F}_P$ is the P-point DFT matrix, and the superscript H denotes the Hermitian conjugate. $\Phi_q^{-1}\breve{\mathbf{H}}_q\Phi_q$ becomes a circulant matrix with first column $\left(\breve{h}_{0,q},W_N^q\breve{h}_{1,q},\ldots,W_N^{(P-1)q}\breve{h}_{P-1,q}\right)$, and the diagonal elements of $\mathbf{D}_q$ equal to the Fourier transform of this column vector.

Based on this diagonalization, a one-tap equalizer can be realized by left multiplying $\breve{\mathbf{y}}_q$ by $\mathbf{F}_P\Phi_q^{-1}$, obtaining

$$\begin{aligned}\mathbf{F}_P\Phi_q^{-1}\breve{\mathbf{y}}_q&=\mathbf{F}_P\Phi_q^{-1}\breve{\mathbf{H}}_q\Phi_q\mathbf{F}_P^H\mathbf{F}_P\Phi_q^{-1}\breve{\mathbf{x}}_q+\mathbf{F}_P\Phi_q^{-1}\breve{\mathbf{n}}_q\\&=\mathbf{D}_q\mathbf{F}_P\Phi_q^{-1}\breve{\mathbf{x}}_q+\mathbf{F}_P\Phi_q^{-1}\breve{\mathbf{n}}_q.\end{aligned} \quad (14)$$

Since the channel matrix $\mathbf{D}_q$ is a diagonal matrix, a one-tap equalizer, such as the zero-forcing (ZF) equalizer, can be realized to remove the channel distortions. As a result of (14), channel estimation can be implemented easily by transmitting carefully chosen training symbols $\breve{\mathbf{x}}_{tr}$ such that $\mathbf{F}_P\Phi_q^{-1}\breve{\mathbf{x}}_{tr}$ is a vector with constant modulus.

In comparison of (14) with $\tilde{\mathbf{y}}_q$, $\tilde{\mathbf{x}}_q$, and $\tilde{\mathbf{h}}_q$, we note the following relationship:

$$\tilde{\mathbf{y}}_q = \mathbf{F}_P\Phi_q^{-1}\breve{\mathbf{y}}_q, \quad \tilde{\mathbf{x}}_q = \mathbf{F}_P\Phi_q^{-1}\breve{\mathbf{x}}_q, \quad \mathrm{diag}(\tilde{\mathbf{h}}_q) = \mathbf{D}_q \tag{15}$$

which shows the connection between the intermediate and the final outputs in the D&C algorithm. Equation (15) suggests that, in an asymmetric OFDM system, part of the IFFT in the transmitter is equivalently shifted to the receiver. In fact, Q P-point IFFTs, each requiring $N/2\log_2 P$ multiplications based on a radix-2 algorithm, are transferred from the transmitter to the receiver. This viewpoint interprets the name of the asymmetric OFDM system and can be used to generalize the system. The presented structure so far has explicit interpretation from the decimation-in-time FFT algorithm. Following the principle of shifting a part of IFFT, asymmetric OFDM systems can be extended to be based on any FFT algorithm, for example, the decimation-in-frequency FFT algorithm.

As a bridging system between OFDM and SC-FDE, asymmetric OFDM provides various trade-offs between system performance, complexity, and power consumption. Adjustable system features include PAPR, frequency sensitivity, hardware complexity and power consumption, and frequency diversity. Compared to OFDM systems, asymmetric OFDM has smaller PAPR, better frequency offset sensitivity (theoretically verifiable), and better frequency diversity. Thanks to the independence of input symbols, the PAPR of signals in asymmetric OFDM systems is proportional to the size of IFFT (the value of Q), similar to that in OFDM systems. The reduced PAPR can be quantified by comparing the PAPR of the outputs from N-point and Q-point IFFTs and could be 0–3 dB, depending on the values of N, P, and the modulation scheme. Compared to SC-FDE, asymmetric OFDM has less unbalanced complexity between transmitter and receiver and is consequently more suitable for distributed networks, where it is preferable for transmitters and receivers to have similar complexity. Due to the extra IFFT operation after single-tap equalization, asymmetric OFDM suffers similar noise enhancement and error propagation problems to SC-FDE. Next, based on a ZF equalizer, we analyze the bit-error rate (BER) performance of asymmetric OFDM systems, including OFDM and SC-FDE sysems, and study how noise enhancement and frequency diversity counteract each other.

A ZF equalizer uses inverse channel coefficients as equalizer taps. Assume the receiver has perfect channel knowledge. According to (14), the estimated signal $\breve{\mathbf{x}}_q$ is given by

$$\langle\breve{\mathbf{x}}_q\rangle = \breve{\mathbf{x}}_q + \Phi_q\mathbf{F}_P^H\mathbf{D}_q^{-1}\mathbf{F}_P\Phi_q^{-1}\breve{\mathbf{n}}_q \tag{16}$$

where $\langle\breve{\mathbf{x}}_q\rangle$ denotes the estimate of $\breve{\mathbf{x}}_q$.

The signal-to-noise power ratio (SNR) of $\langle\breve{\mathbf{x}}_q\rangle$ can be computed as

$$\gamma_q = \frac{\frac{\sigma_x^2}{\sigma_n^2}}{\frac{1}{P}\sum_{p=0}^{P-1}|\tilde{h}_{pQ+q}|^{-2}} \tag{17}$$

where $|x|$ denotes the absolute value of x, and σ_x^2 is the variance of each symbol in $\breve{\mathbf{x}}_q$. Note that we have used the results in (15) and (3) to represent the channel coefficients in $\mathbf{D}_q$. When BPSK modulation is applied, the BER of an asymmetric OFDM symbol (including all $\breve{\mathbf{x}}_q$, $q = 0, \ldots, Q-1$) can be represented as

$$\mathrm{Pe} = \frac{1}{Q}\sum_{q=0}^{Q-1}\mathcal{Q}\left(\sqrt{\frac{\frac{2\sigma_x^2}{\sigma_n^2}}{\frac{1}{P}\sum_{p=0}^{P-1}|\tilde{h}_{pQ+q}|^{-2}}}\right) \tag{18}$$

where $\mathcal{Q}(x) = \int_x^{+\infty}\exp(-t^2/2)dt/\sqrt{2\pi}$. Equation (18) also represents the BER for general OFDM ($P = 1$, $Q = N$) and SC-FDE ($P = N$, $Q = 1$) systems.

From (18), we can see both of the effects of noise enhancement and frequency diversity. On the one hand, any small channel coefficient $\tilde{h}_{pQ+q}$ results in noise enhancement and error propagation in a group of P data symbols. On the other hand, frequency diversity is achieved by averaging the channel power over the same group of symbols. Clearly, in OFDM systems, there is no error propagation and inherent frequency diversity, and limited frequency diversity is achieved by external methods, such as coding.

For the function $\mathcal{Q}\left(\sqrt{2\sigma_x^2/\sigma_n^2/z}\right)$ of z, the second derivative of the function with respect to z is given by

$$\frac{\partial^2\mathcal{Q}}{\partial z^2} = \frac{1}{2}\sqrt{\frac{\frac{\sigma_x^2}{\sigma_n^2}}{\pi z^5}}\left(\frac{\frac{\sigma_x^2}{\sigma_n^2}}{z} - 1.5\right)\exp\left(-\frac{\frac{\sigma_x^2}{\sigma_n^2}}{z}\right). \tag{19}$$

We can see that the function $\mathcal{Q}(\sqrt{2\sigma_x^2/\sigma_n^2/z})$ is convex when $\sigma_x^2/\sigma_n^2/z > 1.5$ and concave when $\sigma_x^2/\sigma_n^2/z < 1.5$. For two asymmetric OFDM systems, one with parameters P_1 and Q_1, and the other with $P_2 = P_1/M$ and $Q_2 = MQ_1$ where $M \geq 1$ and is a power of 2, we can rewrite their BER expressions such that the Jensen's inequality is applicable. According to Jensen's inequality, we can conclude that

$$\begin{aligned}&\mathrm{Pe}_1 > \mathrm{Pe}_2, \text{ if } \frac{\sigma_x^2}{\sigma_n^2} < 1.5z,\\ &\mathrm{Pe}_1 < \mathrm{Pe}_2, \text{ if } \frac{\sigma_x^2}{\sigma_n^2} > 1.5z\end{aligned} \tag{20}$$

where

$$\begin{aligned}&z = \frac{1}{P_2}\sum_{p=0}^{P_2-1}|\tilde{h}_{(p+m/M)Q_2+q}|^{-2}, \quad m = 0, \ldots, M-1\\ &q = 0, \ldots, Q_1 - 1.\end{aligned} \tag{21}$$

The performance bound given by the two inequalities is very loose because the condition needs to be true for any z, as shown in (21). Nevertheless, from the inequalities, we can see the trend that, when SNR is small, asymmetric OFDM systems with smaller P have better BER performance, while with SNR increasing, systems with larger P will become superior. The exact SNR point corresponding to equal performance of two systems depends on the channel condition. Thus, it is straightforward to see the performance difference between asymmetric OFDM, general OFDM, and SC-FDE systems. Although this result is obtained based on a single channel realization, it is meaningful for package systems in quasi-static channels. We will also see from the simulation results that, averaging

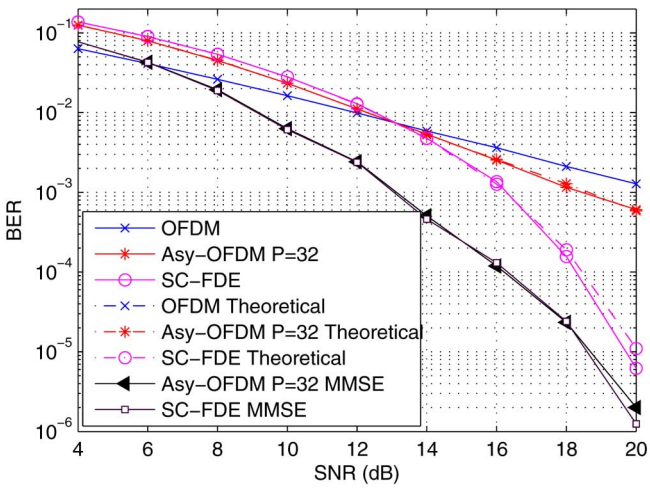

Fig. 2. BER performance for uncoded asymmetric OFDM systems with BPSK modulation, where $P = 1$ (OFDM), $P = 32$, and $P = N = 256$ (SC-FDE).

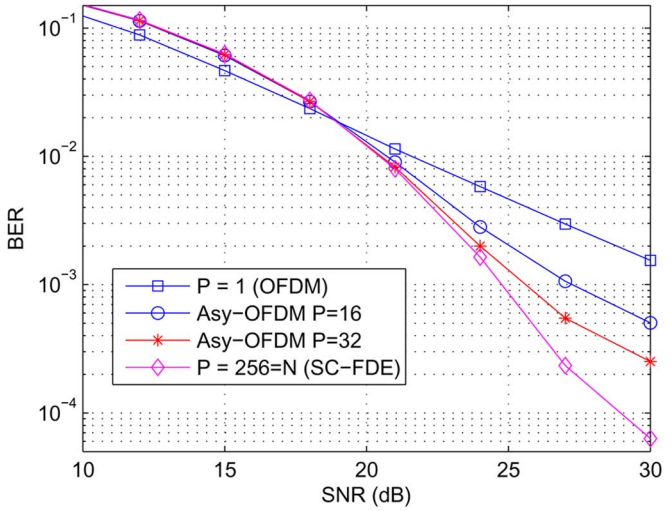

Fig. 3. BER performance for uncoded asymmetric OFDM systems with 16QAM modulation and MMSE equalization where $P = 1$ (OFDM), $p = 16$, $P = 32$, and $P = N = 256$ (SC-FDE).

over hundreds of channel realizations from a specific channel model, the BER comparison of asymmetric OFDM systems with different P gives the same relationship to the analytical results here.

For asymmetric OFDM systems with $P \neq 1$, performance can be significantly improved when advanced equalizers, such as the minimum mean-squared error (MMSE) equalizer, are applied thanks to the reduced noise enhancement effect. It is known that the MMSE equalizer helps general OFDM little because ZF is already the maximum-likelihood estimator for OFDM systems [6]. An MMSE equalizer, given by $w_q = \mathbf{D}_q^H \left(\mathbf{D}_q^H \mathbf{D}_q + \sigma_n^2/\sigma_x^2 \mathbf{I}\right)^{-1}$, has marginally higher complexity by requiring the estimation of noise variance.

IV. Simulation Results

In this section, we present the BER performance of asymmetric OFDM systems, compared with OFDM and SC-FDE systems. The parameter N is fixed at 256. System imperfections such as CFO and PAPR distortions are not introduced in the simulation. In each simulation result, BER is averaged over hundreds of channel realizations.

Fig. 2 shows simulation results for uncoded, BPSK modulated asymmetric OFDM systems with $P = 1$ (OFDM), $P = 32$, and $P = N = 256$ (SC-FDE) systems. The channel model is adopted from HIPERLAN Model E [7], which is a dense indoor multipath channel model with nonline-of-sight conditions. Channel estimation is assumed to be perfect. Fig. 2 shows that simulation results are a good match to the analytical results. We can also see that an MMSE equalizer significantly improves the performance of asymmetric OFDM and SC-FDE.

Fig. 3 shows BER performance for systems with 16QAM modulation. The channel model is adopted from IEEE 802.16, which is an outdoor channel model with a limited number of taps. Channel is estimated using two training symbols based on a ZF algorithm. From Fig. 3, we can see a similar trend, in BER performance of asymmetric OFDM systems with different values of P, to that of Fig. 2 where BPSK modulation is used. In fact, for various modulations including QPSK and 64QAM, in our simulations, we have observed the similar trend and found that asymmetric OFDM systems outperforms OFDM systems at moderate SNR values (smaller than 25 dB) when an MMSE equalizer is applied.

V. Conclusion

In this letter, based on a novel three-layer FFT structure, we developed asymmetric OFDM systems that bridge between OFDM and SC-FDE systems. The asymmetric OFDM systems have reduced PAPR and improved CFO sensitivity and frequency diversity, compared to OFDM systems, and less unbalanced complexity compared to SC-FDE systems. Performance analysis shows that a "bridging" BER is achievable in asymmetric OFDM systems. The asymmetric OFDM scheme provides significant flexibility in system design and operation, and it is particularly promising for distributed networks where transceivers can negotiate link parameters according to their hardware capability and battery status.

References

[1] N. Dinur and D. Wulich, "Peak-to-average power ratio in high-order OFDM," *IEEE Trans. Commun.*, vol. 49, no. 6, pp. 1063–1072, Jun. 2001.

[2] T. Pollet, M. V. Bladel, and M. Moeneclaey, "BER sensitivity of OFDM systems to carrier frequency offset and Wiener phase noise," *IEEE Trans. Commun.*, vol. 43, pp. 191–193, Feb./Mar./Apr. 1995.

[3] D. Falconer, S. Ariyavisitakul, A. Benyamin-Seeyar, and B. Eidson, "Frequency domain equalization for single-carrier broadband wireless systems," *IEEE Commun. Mag.*, vol. 40, no. 4, pp. 58–66, Apr. 2002.

[4] J. G. Proakis and D. G. Manolaki, *Digital Signal Processing: Principles, Algorithms, and Applications*, 3rd ed. Englewood Cliffs, NJ: Prentice-Hall PTR, 1996.

[5] J. C. R. Claeyssen and L. A. dos Santos Leal, "Diagonalization and spectral decomposition of factor block circulant matrices," *Linear Alg. Appl.*, vol. 99, pp. 41–61, Feb. 1988.

[6] Z. Wang, X. Ma, and G. B. Giannakis, "OFDM or single-carrier block transmissions," *IEEE Trans. Commun.*, vol. 52, no. 3, pp. 380–394, Mar. 2004.

[7] Channel Models for Hiperlan/2 in Different Indoor Scenarios, European Telecommunications Standards Institute, Sophia-Antipolis, Valbonne, France, 1998, Norme ETSI, Tech. Rep. doc. 3ERI085B.